**US Army Corps
of Engineers**
Waterways Experiment
Station

HYDRAULICS LAB COPY

3DSALT: A Three-Dimensional Finite Element Model of Density-Dependent Flow and Transport Through Saturated-Unsaturated Media

by Gour-Tsyh Yeh, Jing-Ru Chang,
Jin-Ping Gwo
Pennsylvania State University

Hsin-Chi Lin, David R. Richards,
William D. Martin

Approved For Public Release; Distribution Is Unlimited

The contents of this report are not to be used for advertising, publication, or promotional purposes. Citation of trade names does not constitute an official endorsement or approval of the use of such commercial products.

3DSALT: A Three-Dimensional Finite Element Model of Density-Dependent Flow and Transport Through Saturated-Unsaturated Media

by Gour-Tsyh Yeh, Jing-Ru Chang,
Jin-Ping Gwo

Department of Civil Engineering
Pennsylvania State University
University Park, PA   16802

Hsin-Chi Lin, David R. Richards,
William D. Martin

U.S. Army Corps of Engineers
Waterways Experiment Station
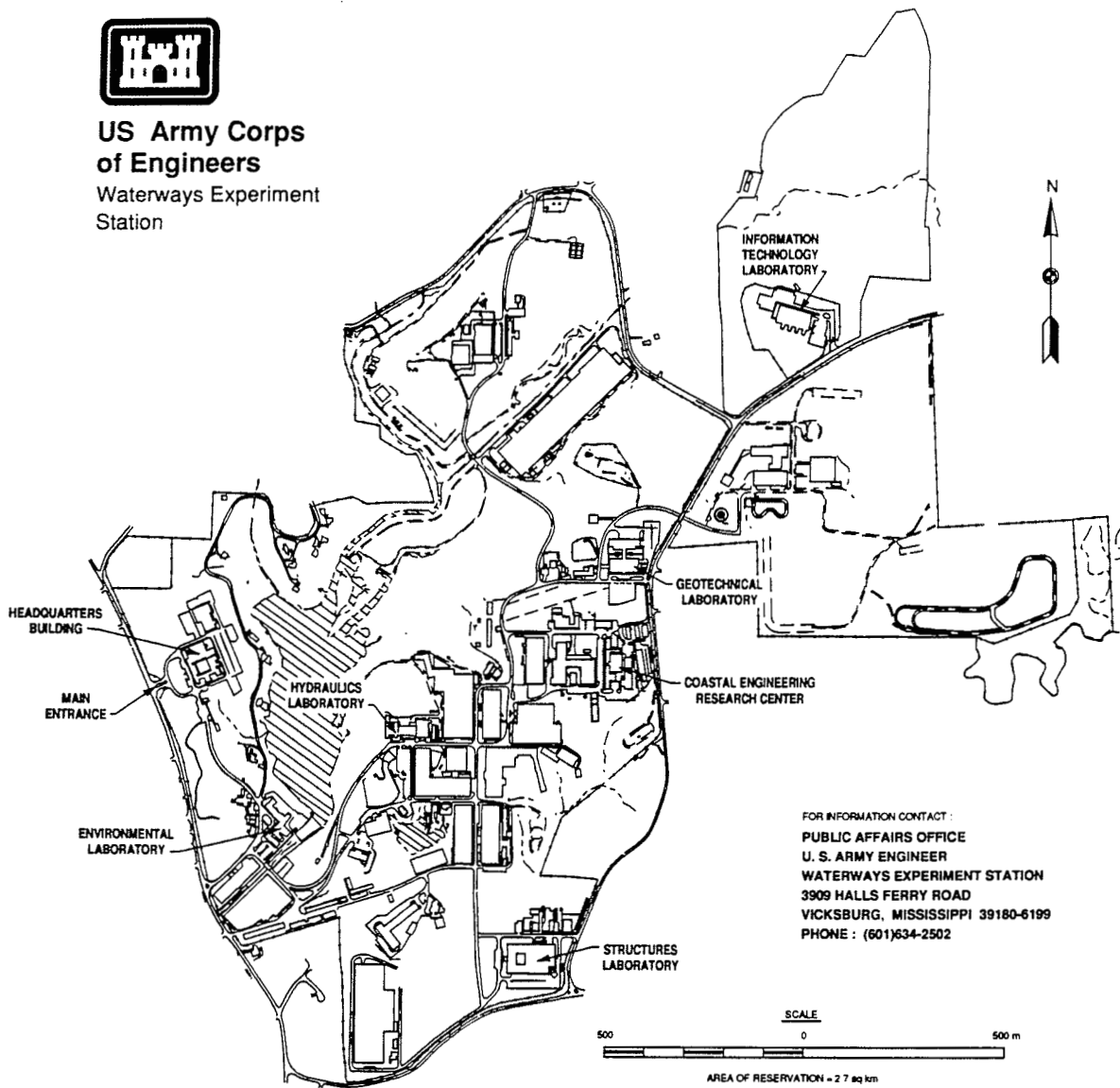3909 Halls Ferry Road
Vicksburg, MS   39180-6199

Final report

**US Army Corps
of Engineers**
Waterways Experiment
Station

N

INFORMATION
TECHNOLOGY
LABORATORY

GEOTECHNICAL
LABORATORY

HEADQUARTERS
BUILDING

COASTAL ENGINEERING
RESEARCH CENTER

MAIN
ENTRANCE

HYDRAULICS
LABORATORY

ENVIRONMENTAL
LABORATORY

FOR INFORMATION CONTACT :
PUBLIC AFFAIRS OFFICE
U. S. ARMY ENGINEER
WATERWAYS EXPERIMENT STATION
3909 HALLS FERRY ROAD
VICKSBURG, MISSISSIPPI 39180-6199
PHONE : (601)634-2502

STRUCTURES
LABORATORY

SCALE

500   0   500 m

AREA OF RESERVATION = 2 7 sq km

Contents

SF 298

List of Figures

Preface

This report on a three-dimensional finite element model of density-dependent flow and transport through saturated-unsaturated media was prepared for the U.S. Army Engineer District, Wilmington.

The study was conducted as part of the Cape Fear Groundwater Modeling Study in the Hydraulics Laboratory (HL) of the U.S. Army Engineer Waterways Experiment Station (WES) during the period November 1992 to April 1993 under the direction of Messrs. F. A. Herrmann, Jr., Director, HL; R. A. Sager, Assistant Director, HL; and W. H. McAnally, Jr., Chief, Estuaries Division (ED), HL.

The report was prepared by Drs. Gour-Tsyh Yeh, Jing-Ru Chang, and Jin-Ping Gwo, Pennsylvania State University; and Dr. Hsin-Chi Lin, Estuarine Engineering Branch (EEB), ED; Mr. David R. Richards, Chief, Estuarine Simulation Branch, ED, and Mr. William D. Martin, Chief, EEB.

At the time of publication of this report, Director of WES was Dr. Robert W. Whalin. Commander was COL Bruce K. Howard, EN.

1   Introduction

Background

Due to population expansion as well as agricultural and industrial growth, pollution of freshwater aquifers is becoming more and more apparent, especially when considering the increasing demand on the quality and quantity of fresh water. Often when a contaminant is introduced into the groundwater system, clear changes in the groundwater density occur that may be sufficiently large to alter the flow dynamics of the system. The pollutant may either displace or mix with the fresh water. The consequence is frequently the degradation or loss of the water resource and the need to seek alternative supplies of fresh water or to purify the polluted water body. The best-known case of such an occurrence is saltwater intrusion. Saltwater intrusion often occurs when, due to the rising demand for fresh water, groundwater is excessively pumped to satisfy this need. The hydraulic gradients that are produced from the excessive pumping may induce a flow of saline water toward the pumping well. Thus, this seawater encroachment can easily upset the long-term natural equilibrium between the fresh water and seawater. Inevitably the seawater wedge moves inland, encroaching on the underground supply of fresh water.

The major causes of saltwater intrusion are overpumping in coastal areas, excessive pumping in noncoastal regions which overlay saline water bodies, advancement of salt water through leaky well casings, and natural sources and processes such as drought or tidal variations (Atkinson et al. 1986). Such encroachment will obviously limit the groundwater for domestic, agricultural, or industrial purposes. Hence, there is a need to predict the location and movement of the saltwater interface in order to be able to protect freshwater aquifers from the possible danger of contamination. Practical management also includes some knowledge of not only the present response, but also of the long-term transient response. For these managerial purposes, a numerical model can easily assist in estimating the location of the salt water for given sets of hydrologic conditions.

In the past, several numerical models have been used to predict the location and movement of the saltwater interface for different types of problems. Depending on the method of treating the interface, these numerical models can

be categorized as the following: (a) sharp interface models and (b) diffused (dispersed) interface models (Contractor and Srivastava 1990). The former type was used to investigate the saltwater interface by a number of researchers (Liu et al. 1981; Henry 1959; Shamir and Dagan 1971; Wilson and Sa da Costa 1982). However, in many cases, the sharp interface assumption is justified only to provide an appropriate simulation under certain conditions, such as when the width of the transition zone is relatively small compared to the thickness of the aquifer. The sharp interface assumption was applied by many investigators since when combined with the Dupuit assumption of horizontal flow, this assumption greatly simplifies the model. Various numerical methods, such as the finite difference methods, finite element methods, and the method of characteristics, have been applied in sharp interface models, some with much success, some with less success. In addition, numerical models based on the boundary integral equation method, assuming an abrupt interface, have been presented (Liggett and Liu 1979; Liu et al. 1981).

Nevertheless, the sharp interface approach can be troublesome when the change in the shape of intrusion is large and/or the aquifer system is complex. This becomes quite apparent when applying the finite element method to the problem of the interface. If, as in the sharp interface approach, the fresh water and salt water are assumed to be immiscible, then certain conditions along the interface boundary must be satisfied. Hence, when the finite element method is applied, the position of the interface must be specified in order to partition each fluid region into individual elements. Needless to say, the finite element method becomes quite difficult in the sharp interface model.

Therefore, a simulation model, such as the diffusive interface model, which accounts for the hydrodynamic effects of dispersion, is much more practical since it gives more details concerning the transition zone, whereas the sharp interface model only represents the overall flow characteristics of the system. Also, the diffusive interface model annihilates the difficulty due to the inner boundary even if the aquifer system is quite complex (Essaid 1990).

As early as 1964, Henry developed the first solution for the steady-state salt distribution in a confined coastal aquifer. He assumed a constant dispersive mechanism in the aquifer and concluded that the steady-state condition is in dynamic equilibrium due to the gravitational forces and dispersion that create a saltwater convection cell. Henry's problem was restated by Lee and Cheng (1974) in terms of stream functions. They formulated a numerical solution which assumed constant dispersion. In 1975, Segol, Pinder, and Gray (1975) developed the first transient solution based on a velocity-dependent dispersion coefficient using the Galerkin finite element method to solve the set of nonlinear partial differential equations describing the movement of a saltwater front in a coastal confined aquifer. Numerous other researchers, such as Pinder and Cooper (1970), Andrews (1981), and more recently Frind (1982a,b), and Huyakorn et al. (1987) have used numerical models for simulation of saltwater intrusion problems using the diffusive interface approach. Some of the numerical diffusive interface models

unfortunately do not consider density-dependent fluid flow and solute transport for mathematical simplification reasons. On the other hand, many models (Pinder and Cooper 1970; Lee and Cheng 1974; Frind 1982a,b; Huyakorn et al. 1987) do. In many cases, however, a steady-state solution in transient simulations was not obtained due to high computing costs.

Adequate knowledge about the physical dynamics of the phenomenon of saltwater encroachment is necessary for the proper management of coastal groundwater resources. Hence, in order to portray the physical complexities and also the temporal and spatial variations involved with saltwater intrusion, the development of numerical models has become quite essential. For this purpose, a Three-Dimensional Finite Element Model for Density-Dependent Flow and Transport Through Saturated-Unsaturated Porous Media (3DSALT) has been developed. This model stems from the combination and modification of two previous codes, a groundwater flow model (FEMWATER, Yeh 1987) and a subsurface contaminant transport model (LEWASTE, Yeh 1992). In the newly combined model, density-dependent effects are accounted for, since according to Reilly and Goodman (1985), it is necessary to consider the sea-water intrusion problem as a density-dependent flow and transport problem in order to account for the dispersed nature of the saltwater-freshwater interface and the associated saltwater circulation zones.

Even though the model, 3DSALT, can be used to investigate saturated-unsaturated flow alone, contaminant transport alone, or combined flow and transport, in this report the code will be used to study seawater intrusion problems, thus using the last option. The code will be verified with similar simulations of other numerical models.

In addition, general facts, such as sources, effects, and control of seawater intrusion, as well as physical and mathematical theory, will be presented to complete this study of saltwater intrusion.

In comparison, sea water is around 2.5 percent heavier than fresh water. Based on the relation, a 12.5-m freshwater column is needed to keep a 12.2-m seawater column in balance. Therefore, within a reasonable distance from the ocean, theoretically every 0.30 m of fresh water above sea level signifies the existence of 12.2 m of fresh water in the aquifer below sea level. To alleviate the endless danger of sea water encroaching inland, the freshwater levels must be maintained as high as practicable above sea level (Atkinson et al. 1986).

Unfortunately, saltwater intrusion in coastal areas occurs all over the world. Investigation of the sources of salt water intrusion is very crucial since saltwater is probably the most common contaminant in fresh water. In the case of coastal aquifers, it arises from a seawater invasion. In all too many cases, human activities are directly or indirectly responsible for saltwater intrusion in coastal environments, which are often heavily urbanized.

According to Atkinson et al. (1986), salt water present in aquifers may derive from the following sources:

a. Seawater, in coastal regions.

b. Seawater that penetrated aquifers during past geological time.

c. Evaporated water residue left over in tidal lagoons, playas, etc.

d. Salt from thin salt beds or salt domes or disseminated in geological formations.

e. Saline wastewaters from human activities.

f. Return flows from irrigated land to stream.

Saltwater intrusion into freshwater aquifers can be influenced in various ways. For example, if the groundwater gradients are reduced or reversed, then denser, saline water can easily take the place of the fresh water. This occurrence is quite common in coastal aquifers, which are hydraulically continuous with the ocean and in which excess well pumping has disturbed the hydrodynamic equilibrium. Another example is when natural barriers separating the fresh water and salt water are removed, or when there is a subsurface disposal of waste salt waters (Atkinson et al. 1986).

Saltwater intrusion can have negative and undesirable effects. Humans may experience health and welfare problems related to decreased water quality. As little as 2 percent of seawater in fresh water can make it undrinkable. Wildlife and fish may also be adversely affected by either high salinity of springs used for watering or high saline runoff. High saltwater content in irrigation waters may decrease crop productivity and make it essential to change to salt-tolerant crops. In addition, salt water can be unacceptable for many industrial purposes (Atkinson et al. 1986).

To control or combat all the possible adverse effects of saltwater intrusion, a control program must be implemented that takes into consideration the type of encroachment, the hydrologic conditions of the region in question, the areal extent of the problem, as well as the specific source(s). The control of saltwater intrusion can be summarized in a general approach of five steps (Atkinson et al. 1986) :

a. Problem definition.

b. Inventory and analysis.

c. Formulation of alternative control plans.

d. Comparative evaluation of control plans.

e. Selection and implementation of controls.

4

The first and probably the most important step to controlling seawater encroachment is locating and defining the magnitude of the problem. Groundwater monitoring can be used for that purpose. After completion of the first step, an inventory of water users is taken to identify patterns, especially if overpumping is occurring. Also, the development of mathematical or numerical models comes about here to help predict and understand the movement of the salt water. The third step involves the formulation of various alternative seawater intrusion control plans. The fourth step involves the comparative evaluation of control plans, in other words, to investigate if the water quality cannot be brought to the desired levels by other methods than control. The last step involves the formulation of legal and institutional considerations in order to implement the selected method of control (Atkinson et al. 1986).

According to Atkinson et al. (1986), the objective of seawater intrusion control depends on the planned function of water and involves one of the following:

a. Partial or complete avoidance of fresh water migrating seaward.

b. Increasing the rate of flow within the aquifer or the size of the freshwater lens by increasing the freshwater pressures.

c. Preserving a state of seawater intrusion that will not further encroach on the freshwater supply by controlling several methods of freshwater withdrawal in given regions.

In order to meet these objectives, the following methods can be applied in the control of seawater intrusion (Atkinson et al. 1986):

a. Directly recharge the aquifer.

b. Reduce or, in some cases, eliminate pumping.

c. Relocate or disperse pumping wells.

d. Form a hydraulic barrier by recharging fresh water into pumping wells parallel to the coast.

e. Remove encroaching salt water by constructing a trough parallel to the coast.

f. Remove seawater before it reaches the pumping well.

g. Create impermeable subsurface barriers.

h. Combine extraction/injection techniques.

Just which control technique to use in which case can be summarized in Table 1.1 (Bowen 1986).

Table 1.1
Techniques of Saltwater Control

Cause of Intrusion	Control Techniques
Saltwater in a coastal aquifer	Alteration of the pumping pattern Injection freshwater well Injection barrier Extraction barrier Subsurface barrier
Upconing	Alternation of the pumping pattern Saline removing wells
Defective well casing	Plugging defective wells
Saline water zones in freshwater aquifers	Relocating and designing wells
Surface infiltration	Eliminating the surface source
Oil field brine	Injection wells Eliminating surface disposal

There are various hydrogeologic conditions in coastal aquifers. Some of the most common examples are depicted in Figure 1.1 (Essaid 1990). Figures 1.1(a) and (b) portray an unconfined aquifer with an impermeable bottom and an unconfined island aquifer with a free bottom, respectively, whereas Figure 1.1(c) shows a coastal confined aquifer.

Figure 1.2 depicts an idealized cross section of a layered coastal aquifer under steady-state and transient conditions. In the steady-state case (Figure 1.2(a)), there is a stable seaward hydraulic gradient within each aquifer. The location and shape of a stationary "interface" between the fresh water and salt water is determined by the freshwater potential and gradient. As the seawater flows in from the sea within every aquifer layer, a wedge-shaped body of denser salt water settles underneath the lighter fresh water. Fresh water in the lower (confined) aquifers may leak upward through the overlying layers and/or discharge through the outcrop, while fresh water in the top (unconfined) aquifer discharges to the sea via the ocean floor. In a system, such as Figure 1.2(a), the zone of mixed fresh water and salt water will not be static since there might be fresh water leaking vertically upward into an overlying saltwater zone. However, if the system were of a one-layer aquifer configuration, the seawater would be nearly static.

On the other hand, in the transient case (Figure 1.2(b)), salt water may flow into the aquifer system by leaking into the confining layers as well as ocean floor and/or by entering through the outcrop. Gradually the "interface" will move inland and encroach on the freshwater supply. Hence, the dynamics of both the freshwater and saltwater domains must be investigated in order to get a complete picture of the seawater intrusion in coastal aquifers, especially when developing numerical models for saltwater intrusion problems (Essaid 1990).
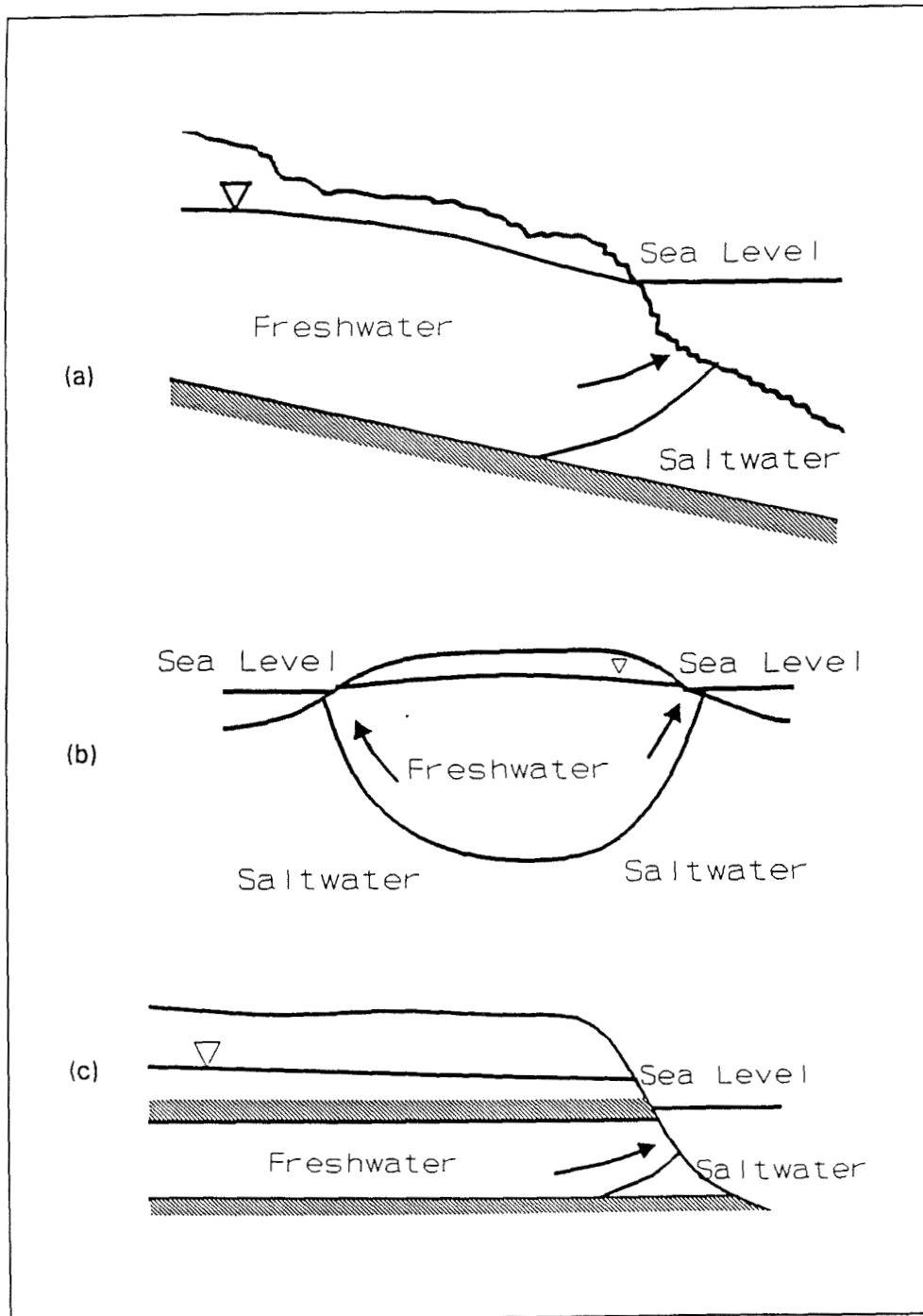
Figure 1.1. Common examples of hydrogeological conditions in coastal aquifers (from Essaid 1990)
(a) Phreatic aquifer with an impermeable bottom
(b) Phreatic island aquifer with a free bottom
(c) Confined aquifer
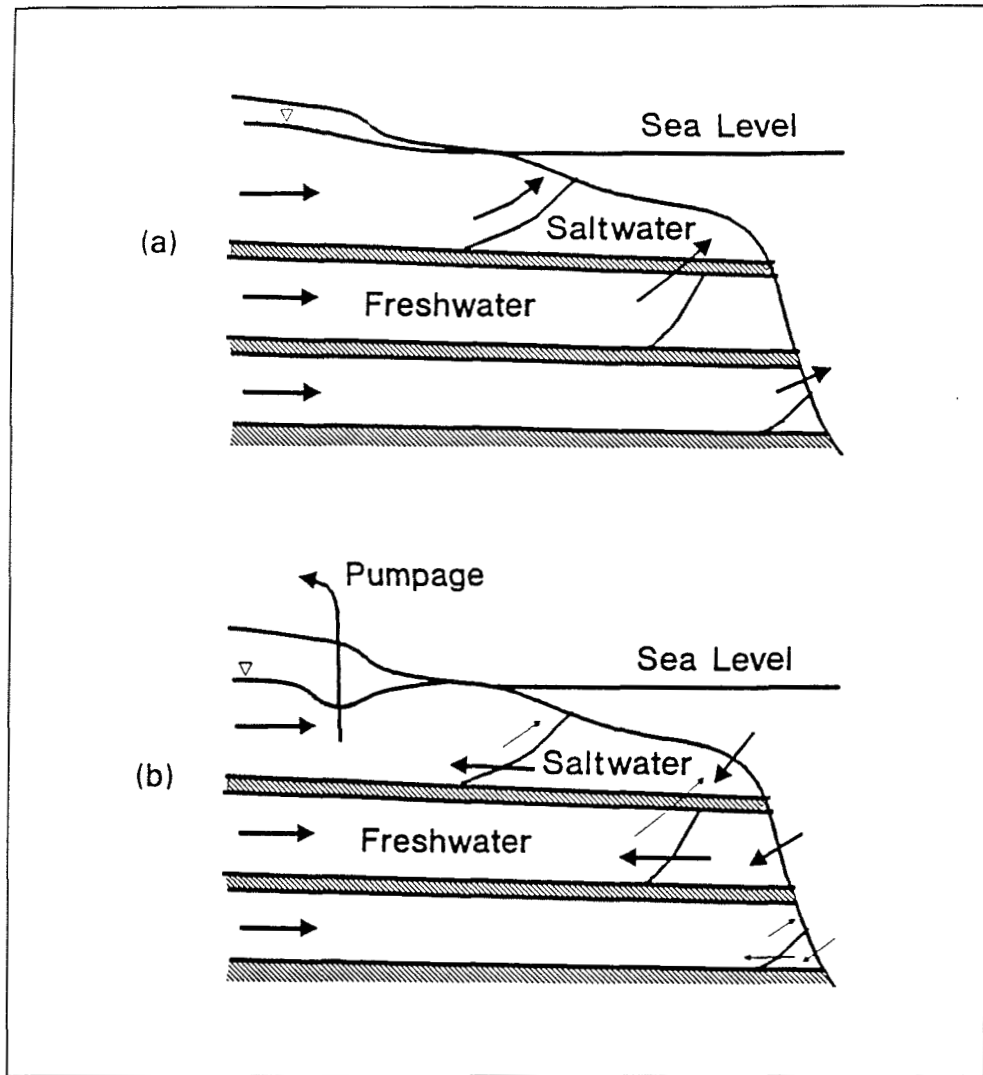
Figure 1.2. Idealized cross-sections of a layered coastal aquifer (from
             Essaid 1990)
             (a) Steady-state case
             (b) Transient case

In the freshwater region of coastal aquifers, the flow can sometimes be
easily altered by inland changes of discharge or recharge. If the freshwater
flow towards the sea is reduced by some means, this may cause the
freshwater-saltwater interface to migrate landward, thus resulting in saltwater
intrusion into the aquifer. On the other hand, if the freshwater flow towards
the sea is increased, the interface may be forced to move towards the sea.
Nevertheless, the rate of the interface movement as well as the transient
aquifer head response will be determined by the properties of the aquifer and
the boundary conditions on both sides of the interface. Generally, the changes
in inland freshwater discharge that determine the rate of the interface
movement in the aquifer affect the freedom of the salt water to move into or

8

out of a coastal aquifer system. Hence, it is very important to examine the interface and describe its properties in a realistic fashion (Essaid 1990).

Both disperse and sharp interface approaches have been used by numerous researchers to study saltwater intrusion in coastal aquifers via numerical models. However, as also discussed, the sharp interface approach may be an adequate first approximation in some cases, but in may other cases, the zone of dispersion might be quite extensive, making the sharp interface approach a very poor approximation. In some studies, such as field observations in the Biscayne aquifer, Florida, for example, the error of using a sharp instead of a disperse interface approach can be as much as a few miles seaward. Such an error clearly demonstrates that a sharp interface model cannot fully represent the nature of saltwater intrusion, at least not for some coastal aquifers that experience a thick mixing zone generated by freshwater and saltwater dispersion (Lee and Cheng 1974). In addition, it has been revealed by actual measurements that the dispersion-diffusion phenomena may heavily contribute to notable fluctuations of the water table in coastal aquifers (De Wiest 1965).

One of the early researchers, Beran (1955), investigating the freshwater-saltwater interface, described three cases of flow: (a) when the effects of molecular diffusion are prevailing; (b) when the randomness of the flow pattern is as significant as the molecular diffusion in the mixing process; (c) when the effects of randomness of the flow pattern and molecular diffusion are insignificant (Sherif, Singh, and Amer 1990).

As stated, in reality, where the fresh water and salt water merge, a dispersion zone of finite thickness occurs due to the effects of hydrodynamic dispersion (mechanical dispersion and molecular diffusion). No distinct interface exists since the fresh water and sea water are considered soluble in each other. This transition zone also is influenced by the action of tides and well pumping. Maximum widths of the transition zone occur in extremely permeable coastal aquifers that are exposed to heavy pumping. According to Volker and Rushton (1982), the extent of the dispersion zone is dependent on numerous factors, such as the dispersion parameters of the coastal aquifer and the rate of discharge of the groundwater, as well as the relative densities of the fresh water and salt water. In this dispersion zone, the concentration and thus the fluid density vary. Dispersion results in a change of concentration of the displacing fluid in the transition zone, basically due to the fact that individual fluid particles travel at variable velocities through the irregularly and randomly shaped pore channels of the medium. The flow pattern in the aquifer will obviously be altered by this transition zone. Since the transition zone is moving towards the sea, the saline water coming from underlying sources flows in the same direction. Therefore, due to continuity, the flow is inland in the saltwater region. In addition, the groundwater salinity increases with depth from that of fresh water to that of salt water in the transition zone (Bowen 1986).

Figure 1.3 illustrates the transition zone between the fresh water and salt water in a coastal aquifer. It can be seen that the salt water tends to force
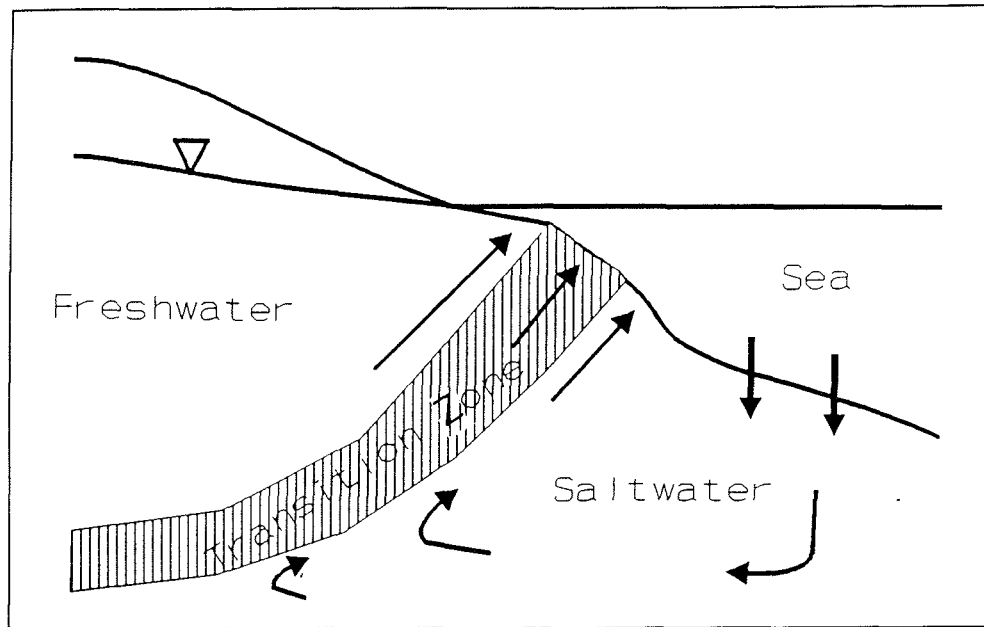
Figure 1.3. Illustration of transition zone and circulation (from Essaid 1990)

itself underneath the fresh water due to the higher density of the salt water. The "diluted" salt water ascends and moves towards the sea along the interface due to the fact that it is less dense than the original seawater. The transfer of salts out of the saltwater environment induces circulation. Due to this movement, there exists a cyclic flow of saltwater originating from the sea, across the ocean floor, to the transition zone, and back to the sea. Even under steady-state conditions, this cyclic flow is evident (Essaid 1990).

The model developed in this research is designed to solve a system of governing equations pertaining both to flow and transport through saturated-unsaturated media. Numerical simulation of contaminant transport in subsurface systems involves the solution of two partial differential equations. The first differential equation is the flow equation that describes the head distribution in the aquifer of interest. For the developed model, the classically used pressure head variable employed in the fluid continuity equation of many flow modules was replaced by the use of equivalent freshwater head that generally results in the elimination of static quantities and the improvement of numerical efficiency (Frind 1982b). If the head distribution is known, then the flow can be calculated via Darcy's law. The other differential equation is the transport (dispersion) equation which is used to describe the chemical concentration. In the specific case of saltwater intrusion, a constitutive equation that relates fluid density to concentration is also needed (Galeati, Gambolati, and Neuman 1992). Furthermore, the two partial differential equations are coupled in such a way that makes, for instance, the seawater intrusion problem nonlinear. Buoyancy effects that cause the upward movement of the fresh water and sea water near the coast primarily affect the degree of nonlinearity (Huyakorn et al. 1987). The coupling is solved in such a way that the groundwater flow and solute transport equations are solved independently and linked through

10

iterations. In addition, initial and boundary conditions must be accounted for when solving this system of governing equations.

Purpose

The purpose of this report is to provide guidance for users to use the 3DSALT model for site-specific application especially for salt intrusion problems in coastal areas.

3DSALT (A Three-Dimensional Finite Element Model of Density-Dependent Flow And Transport Through Saturated-Unsaturated Media) can be used to investigate saturated-unsaturated flow alone, contaminant transport alone, combined flow and transport, or salt intrusion problems in subsurface media. For the flow module, the Galerkin finite element method is used to discretize the Richards equation; and for the transport module, the hybrid Lagrangian-Eulerian finite element method is used to discretize the transport equation. Using the hybrid Lagrangian-Eulerian approach completely eliminates numerical oscillation due to advection transport. Large time-step sizes can be used to overcome excessive numerical dispersion. The only limitation on the size of time-step is the requirement of accuracy with respect to dispersion transport, which does not pose severe restrictions.

Scope

The scope of this report is to derive and solve the governing equations for density-dependent flow and transport in saturated-unsaturated media. The report also provides the description of a main program and subroutines. Three sample problems were provided to illustrate the application of using the model.

The section "Purpose of 3DSALT," Chapter 2, lists the governing equations and describes initial and boundary conditions for which 3DSALT is designed to provide solutions. The section "Description of 3DSALT Subroutines," Chapter 2, contains the description of all subroutines in 3DSALT. This should facilitate the understanding of the code structure by the users. Since occasions may arise when the users have to modify the code, this section should help them to trace the code so they can make necessary adjustments for their purposes. General information on input parameters required by each subroutine is also provided. The section "Parameter Specifications," Chapter 3, contains the parameter specification. For each application, users must assign 58 maximum control-integers. The section "Soil Property Function Specifications," Chapter 3, describes soil property function specifications so that the users will be able to modify subroutine SPRO for each site-specific application. The section "Input and Output Devices," Chapter 3, describes files required for the execution of 3DSALT. Appendix A contains the data input guide that is essential for any site-specific application.

The users may choose whatever units they want to use provided they are maintained in all the input. Units of mass (M), length (L), and time (T) are indicated in the input description.

The special features of 3DSALT are its flexibility and versatility in modeling a range of real-world problems. The model is designed to do the following:

a. Treat heterogeneous and anisotropic media consisting of as many geologic formations as desired.

b. Consider both distributed and point sources/sinks that are spatially and temporally dependent.

c. Accept the prescribed initial conditions or obtain them by simulating a steady-state version of the system under consideration.

d. Deal with transient Dirichlet boundary conditions.

e. Handle time-dependent fluxes due to the gradient of pressure head or concentration varying along the Neumann boundary.

f. Treat time-dependent total fluxes distributed over the Cauchy boundary.

g. Automatically determine variable boundary conditions of evaporation, infiltration, or seepage on the soil-air interface for the flow module and variable boundary conditions of inflow and outflow for the transport module.

h. Include the off-diagonal hydraulic conductivity components in Richards equation for dealing with cases when the coordinate system does not coincide with the principal directions of the hydraulic conductivity tensor.

i. Give three options for estimating the nonlinear matrix.

j. Include two options (successive subregion block iterations and successive point iterations) for solving the linearized matrix equations.

k. Provide two options of treating the mass matrix — consistent and lumping.

l. Provide three adsorption models in the transport module — linear isotherm and nonlinear Langmuir and Freundlich isotherms.

m. Automatically reset time-step size when boundary conditions or source/sinks change abruptly.

12

n. Check the mass balance computation over the entire region for every time-step.

Appendix B provides the physical bases and mathematical foundation for describing density-dependent flow and material transport. Appendix C gives the numerical detail in approximating the governing equations. Readers who wish to comprehend salt intrusion problems and understand numerical approaches should read these two appendices. For practitioners they may be skipped.

2 The 3DSALT Program Structure

Purpose of 3DSALT

3DSALT is designed to solve the following system of governing equations along with initial and boundary conditions, which describe flow and transport through saturated-unsaturated media. The governing equations for flow are basically the modified Richards equation, which is derived in Appendix B.

Governing flow equation

$$\frac{\rho}{\rho_o}\frac{d\theta}{dh}\frac{\partial h}{\partial t} = \nabla\cdot\left[\mathbf{K}\cdot\left[\nabla h + \frac{\rho}{\rho_0}\nabla z\right]\right] + \frac{\rho^*}{\rho_0}q \tag{2.1}$$

where h is the pressure head, t is time, $\mathbf{K}$ is the hydraulic conductivity tensor, z is the potential head, q is the source and/or sink, ρ is the water density at chemical concentration C, ρ_0 is the referenced water density at zero chemical concentration, ρ^* is the density of either the injection fluid or the withdrawn water, and θ is the moisture content. The hydraulic conductivity $\mathbf{K}$ is given by

$$\mathbf{K} = \frac{\rho g}{\mu}\mathbf{k} = \frac{(\rho/\rho_o)}{(\mu/\mu_o)}\frac{\rho_o g}{\mu_o}\mathbf{k}_s k_r = \frac{\rho/\rho_o}{\mu/\mu_o}\mathbf{K}_{so}k_r \tag{2.2a}$$

where μ is the dynamic viscosity of water at chemical concentration C; μ_0 is the referenced dynamic viscosity at zero chemical concentration; $\mathbf{k}$ is the permeability tensor; $\mathbf{k}_s$ is the saturated permeability tensor; k_r is the relative permeability or relative hydraulic conductivity; $\mathbf{K}_{so}$ is the referenced saturated hydraulic conductivity tensor. The referenced value is usually taken at zero

chemical concentration. The density and dynamic viscosity of water are functions of chemical concentration and are assumed to take the following form

$$\frac{\rho}{\rho_o} = a_1 + a_2 C + a_3 C^2 + a_4 C^3 \tag{2.2b}$$

and

$$\frac{\mu}{\mu_o} = a_5 + a_6 C + a_7 C^2 + a_8 C^3 \tag{2.2c}$$

where a_1, a_2, ..., a_8 are the parameters used to define concentration dependence of water density and viscosity and C is the chemical concentration.

The Darcy velocity is calculated as follows

$$V = -\mathbf{K} \cdot \left[\frac{\rho_o}{\rho} \nabla h + \nabla z \right] \tag{2.3}$$

Initial conditions for flow equation

$$h = h_i(x,y,z) \quad in \quad R, \tag{2.4}$$

where R is the region of interest and h_i is the prescribed initial condition, which can be obtained by either field measurements or by solving the steady-state version of Equation 2.1.

Boundary conditions for flow equations

Dirichlet conditions:

$$h = h_d(x_b, y_b, z_b, t) \quad on \quad B_d \tag{2.5}$$

Neumann conditions:

$$-\boldsymbol{n} \cdot \boldsymbol{K} \cdot \frac{\rho_o}{\rho} \nabla h = q_n(x_b, y_b, z_b, t) \qquad on \quad B_n, \tag{2.6}$$

Cauchy conditions:

$$-\boldsymbol{n} \cdot \boldsymbol{K} \cdot \left[\frac{\rho_o}{\rho} \nabla h + \nabla z \right] = q_c(x_b, y_b, z_b, t) \qquad on \quad B_c, \tag{2.7}$$

Variable conditions during precipitation period:

$$h = h_p(x_b, y_b, z_b, t) \qquad on \quad B_v \tag{2.8a}$$

or

$$-\boldsymbol{n} \cdot \boldsymbol{K} \cdot \left[\frac{\rho_o}{\rho} \nabla h + \nabla z \right] = q_p(x_b, y_b, z_b, t) \qquad on \quad B_v, \tag{2.8b}$$

Variable conditions during nonprecipitation period:

$$h = h_p(x_b, y_b, z_b, t) \qquad on \quad B_v, \tag{2.8c}$$

or

$$h = h_m(x_b, y_b, z_b, t) \qquad on \quad B_v, \tag{2.8d}$$

or

$$-\boldsymbol{n} \cdot \boldsymbol{K} \cdot \left[\frac{\rho_o}{\rho} \nabla h + \nabla z \right] = q_e(x_b, y_b, z_b, t) \qquad on \quad B_v, \tag{2.8e}$$

where (x_b, y_b, z_b) is the spatial coordinate on the boundary; $\boldsymbol{n}$ is an outward unit vector normal to the boundary; h_d, q_n, and q_c are the prescribed Dirichlet functional value, Neumann flux, and Cauchy flux, respectively; B_d, B_n, and B_c

are the Dirichlet, Neumann, and Cauchy boundaries, respectively; B_v is the variable boundary; h_p is the allowed ponding depth; and q_p is the throughfall of precipitation, respectively, on the variable boundary; h_m is the allowed minimum pressure on the variable boundary; and q_e is the allowed maximum evaporation rate on the variable boundary, which is the potential evaporation. Only one of Equations 2.8a through 2.8e is used at any point on the variable boundary at any time.

The governing equations for transport are derived based on the continuity of mass and flux laws as given in Appendix B. The major processes are advection, dispersion/diffusion, adsorption, decay, and source/sink.

Governing equations for transport

$$\theta \frac{\partial C}{\partial t} + \rho_b \frac{\partial S}{\partial t} + V \cdot \nabla C = \nabla \cdot (\theta D \cdot \nabla C) - \lambda(\theta C + \rho_b S) + QC_{in}$$
$$- \left[\frac{\rho^*}{\rho} Q - \frac{\rho_o}{\rho} V \cdot \nabla \left[\frac{\rho}{\rho_o} \right] \right] C \tag{2.9}$$

$$S = K_d C \quad \text{for linear isotherm} \tag{2.10a}$$

$$S = \frac{S_{max} K C}{1 + KC} \quad \text{for Langmuir isotherm} \tag{2.10b}$$

$$S = KC^n \quad \text{for Freundlich isotherm} \tag{2.10c}$$

where θ is the moisture concentration, ρ_b is the bulk density of the medium (M/L^3), C is the material concentration in aqueous phase (M/L^3), S is the material concentration in adsorbed phase (M/M), t is time, V is the discharge, ∇ is the del operator, D is the dispersion coefficient tensor, λ is the decay constant, Q is the source rate of water, C_{in} is the material concentration in the source, K_d is the distribution coefficient, S_{max} is the maximum concentration allowed in the medium in the Langmuir nonlinear isotherm, n is the power index in the Freundlich nonlinear isotherm, and K is the coefficient in the Langmuir or Freundlich nonlinear isotherm.

The dispersion coefficient tensor D in Equation 2.9 is given by

$$\theta D = a_T |V| \delta + (a_L - a_T) VV/|V| + \theta a_m \tau \delta \tag{2.11}$$

where $|V|$ is the magnitude of V, δ is the Kronecker delta tensor, a_T is lateral dispersivity, a_L is the longitudinal dispersivity, a_m is the molecular diffusion coefficient, and τ is the tortuosity.

Initial conditions for transport:

$$C = C_i(x,y,z) \quad in \quad R \tag{2.12}$$

Prescribed concentration (Dirichlet) boundary conditions:

$$C = C_d(x_b,y_b,z_b,t) \quad on \quad B_d \tag{2.13}$$

Variable boundary conditions:

$$n \cdot (VC - \theta D \cdot \nabla C) = n \cdot VC_v(x_b,y_b,z_b,t) \; if \; n \cdot V \le 0 \tag{2.14a}$$

$$n \cdot (-\theta D \cdot \nabla C) = 0 \; if \; n \cdot V > 0 \tag{2.14b}$$

Cauchy boundary conditions:

$$n \cdot (VC - \theta D \cdot \nabla C) = q_c(x_b,y_b,z_b,t) \quad on \quad B_c \tag{2.15}$$

Neumann boundary conditions:

$$n \cdot (-\theta D \cdot \nabla C) = q_n(x_b,y_b,z_b,t) \quad on \quad B_n \tag{2.16}$$

where C_i is initial concentration; R is the region of interest; (x_b,y_b,z_b) is the spatial coordinate on the boundary; **n** is an outward unit vector normal to the boundary; C_d and C_v are the prescribed concentration on the Dirichlet boundary and the specified concentration of water through the variable boundary, respectively; B_d and B_v are the Dirichlet and variable boundaries, respectively; q_c and q_n are the prescribed total flux and gradient flux through the Cauchy and Neumann boundaries B_c and B_n, respectively.

Since the hybrid Lagrangian-Eulerian approach is used to simulate Equation 2.9, it is written in the Lagrangian-Eulerian form as

$$\left[\theta + \rho_b \frac{ds}{dc}\right] \frac{D_{V_d} C}{Dt} = \nabla \cdot (\theta D \cdot \nabla C) - \lambda(\theta C + \rho_b S) + QC_{in}$$
$$- \left[\frac{\rho^*}{\rho Q} - \frac{\rho_o}{\rho} V \cdot \nabla \left(\frac{\rho}{\rho_o}\right)\right] C \qquad (2.17a)$$

$$V_d = \frac{V}{\theta + \rho_b K_d} \quad \text{for linear isotherm model} \qquad (2.17b)$$

$$\theta \frac{D_{V_f} C}{Dt} + \rho_b \frac{dS}{dC} \frac{\partial C}{\partial t} = \nabla \cdot (\theta D \cdot \nabla C) - \lambda(\theta C + \rho_b S) + QC_{in}$$
$$- \left[\frac{\rho^*}{\rho} Q - \frac{\rho_o}{\rho} V \cdot \nabla \left(\frac{\rho}{\rho_o}\right)\right] C \qquad (2.18a)$$

$$V_f = \frac{V}{\theta} \quad \text{for Freundlich and Langumir models} \qquad (2.18b)$$

where V_d and V_f are the retarded and fluid pore velocities, respectively; and $D_{V_d}()/dt$ and $D_{V_f}()/dt$ denote the material derivative of ( ) with respect to time using the retarded and fluid pore velocities, respectively.

The flow equation (2.1) subject to initial and boundary conditions (Equations 2.5 through 2.8) is solved with the Galerkin finite element method. The transport equations (Equations 2.17 or 2.18) subject to initial and boundary conditions (Equations 2.12 through 2.16) are solved with the hybrid Lagrangian-Eulerian finite element methods. Detail implementation of the numerical approximation of flow and transport problems are given in Appendix C.

Description of 3DSALT Subroutines

3DSALT consists of a MAIN program and 57 subroutines. The program structure of 3DSALT is illustrated in Figure 2.1. The functions of the MAIN program and the subroutines are described below.

Program MAIN

The MAIN is used to specify the sizes of all arrays. The flow of data input for the model is also anchored by the MAIN. The subroutine RDATIO is called to read the geometric and material data. MAIN then calls subroutine PAGEN to generate pointer arrays; SURF to identify the boundary sides and